CONSTRUCTION SOLUTIONS FOR NON-CONTACT LAP SPLICES IN CONCRETE BLOCK CONSTRUCTION

A. Kisin[1] and L.R. Feldman[2]

[1] M.Sc. Student, Department of Civil &Geological Engineering, University of Saskatchewan, Saskatoon, SK, S7N 5A9, Canada, alk102@mail.usask.ca

[2] Associate Professor, Department of Civil &Geological Engineering, University of Saskatchewan, Saskatoon, SK, S7N 5A9, Canada, lisa.feldman@usask.ca

ABSTRACT

A study completed by Ahmed and Feldman concluded that the tensile capacity of non-contact lap splices, where the lapped bars are in adjacent cells, is 29.3% less than contact lap splices of the same length in masonry assemblages. An experimental program was initiated to evaluate remedial measures that may enhance the tensile capacity of non-contact lap splices such that they can achieve a similar tensile resistance to lap splices where the bars are in contact. Three different remedial techniques were evaluated to explore the effects of adding additional confinement or knockout webs within the splice region. In addition, wall splice specimens featuring standard contact and unaltered non-contact lap splices were constructed as controls. Specimens were tested horizontally under monotonic, four-point loading. The effectiveness of the remedial techniques was determined by visual observations of the resulting distress and an analysis of the measured quantifiable data.

Three courses of knock-out webs within and adjacent to the lap splice length was the highest performing remedial technique in terms increasing the tensile capacity of the lapped bars. The decreased coefficient of variation, which also resulted, can be attributed to the elimination of poor bond at the grout-block interface between the lapped bars and prevented splitting from occurring. However, this remedial technique only managed to achieve 58.9% of the tensile capacity of specimens featuring contact lap splices, leaving further remedial methods to be explored.

KEYWORDS: bond, lap splices (contact & non-contact), concrete block construction, mitigative construction techniques, web knock-outs, wall splice specimens

INTRODUCTION

Non-contact lap splices are permitted by CSA S304.1-04 [1] without any adjustment to the required lap splice length, and are frequently provided intentionally, adjacent to door and window openings, and unintentionally, due to alignment errors, in masonry construction. A significant challenge arises when dowels in reinforced concrete grade beams are improperly placed, and fail to line up with the intended reinforced cells in a masonry wall that is to be constructed above. In such cases, the lap splice length is governed by the length of the dowel extending above the grade beam. The traditional remedy in such situations results in non-contact lap splices, where the lapped bars are placed in adjacent cells of the concrete masonry units with no increase in lap splice length; however, a recent investigation by Ahmed and Feldman [2] has

shown that a significant reduction in splice capacity results. Appropriate technical and cost effective means of resolving such cases in a satisfactory manner are required.

The separation of the lapped reinforcement in non-contact lap splices requires the tensile forces carried by one bar to be transferred through the masonry assemblage to the other lapped bar. Sagan et al.'s [3] research of non-contact lap splices in reinforced concrete construction showed that the force transfer between lapped bars which are not in contact can be modelled by a planar truss. This model can also be applied to reinforced masonry construction. Figure 1 shows that the longitudinal force along the bars resists the tension within the reinforcement while the diagonal compressive struts, which are similar to the webs of a plane truss, transfer the tensile forces between the lapped bars. However, Ahmed and Feldman [2] noted that grout shrinkage during curing caused a separation from the concrete masonry unit, resulting in a poor bond between the two materials. Bischoff and Moxon [4] also noted that excessive shrinkage in the grout used to fill the masonry cells led to restrained shrinkage cracking which affected member behaviour. This behaviour hindered the formation of the diagonal compressive struts and reduced the tensile capacity of the lapped bars.

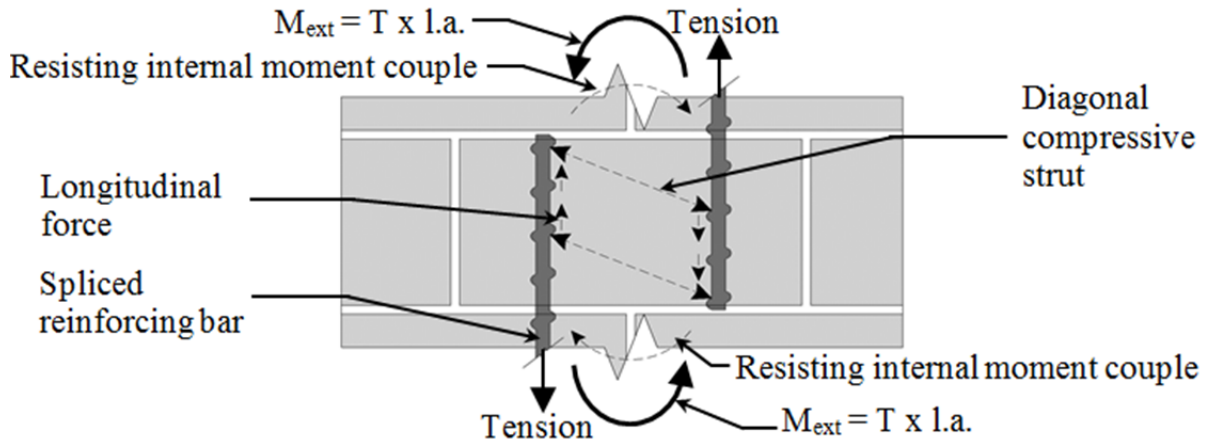

Figure 1: Force Transfer Mechanism Between Lapped Bars in Non-Contact Lap Splices

Figure 1 also shows the separation of the bars results in a lever arm (l.a.) between the tensile forces in the spliced reinforcing bars (T), thus creating an external moment (M_{ext}). This external moment must be resisted by an internal moment which forms between the lapped bars; the capacity of which is largely dependent on the confinement provided by the in-plane stiffness of the surrounding masonry assemblage's geometry and mass. The relatively small-scale double pull-out specimens tested by Ahmed and Feldman [2] required the exterior bar in each lap splice to be located in the cell adjacent to the side face of the specimen. This limited the available lateral confinement. Splitting of the specimens resulted before bond failure could be achieved as a result of poor bond between the grout and the concrete blocks. Wall splice specimens tested in the same investigation [2] showed evidence of splitting cracks, though this was not the primary cause of failure. In practice, masonry walls typically extend laterally in both directions away from the splice location and so may provide additional confinement to enhance the capacity of non-contact lap splices.

A review of the available literature suggests that Ahmed and Feldman's [2] investigation is the sole work which examined the bond behaviour of non-contact lap splices in masonry walls, where the lapped reinforcing bars are located in adjacent cells. The results of this investigation suggest that it is necessary to investigate methods to improve the resistance of non-contact lap splices. This paper discusses the initial results of such an experimental program.

TEST SPECIMENS

Two sets of control wall splice specimens were required to adequately compare the performance of the three proposed remedial techniques. One set of control specimens featured non-contact lap splices, where the lapped bars were placed in adjacent cells. The other set of control specimens featured contact lap splices, where the bars were fastened together using tie wire, to model an ideal splice situation. The results from the two sets of control wall specimens were used as a benchmark to evaluate the efficiency of the three remedial techniques. Three replicate specimens were included in each set of control specimens and all three remedial procedures.

Figure 2 shows the elevations for: the control wall splice specimens with non-contact lap splices (NCLS) (Figure 2 (a)), the control wall splice specimens with contact lap splices (CLS) (Figure 2 (b)), and the remedial wall splice specimens with grouted confinement cells (GCC) (Figure 2 (c)). The remaining two remedial wall splice specimen types have similar profiles to that shown in Figure 2 (a) with additional details of the remediation measures specifically shown in Figure 3. The 13 course tall specimens were constructed in a running bond pattern and all of the cells for all control and remedial technique specimen groups were fully grouted.

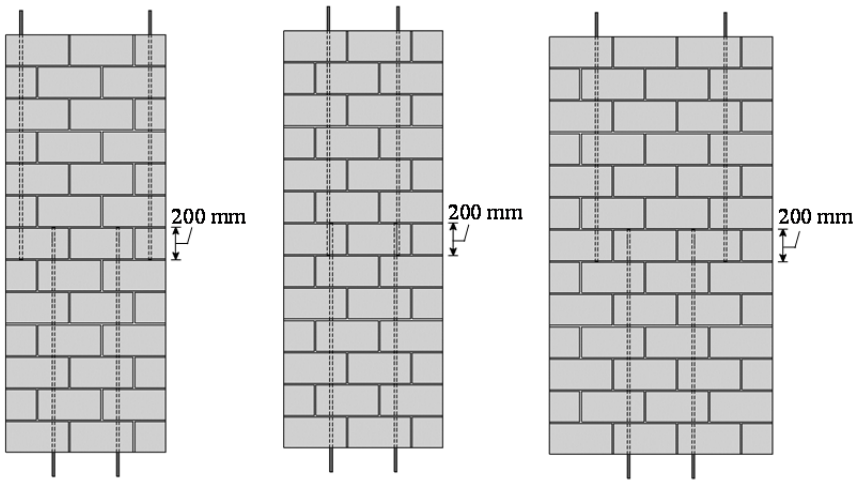

Figure 2: Wall Elevations: (a) NCLS, (b) CLS, and (c) GCC Specimens.

No. 15 deformed bars were used to reinforce all specimens since the results of several previous investigations [2,5] were reinforced exclusively with bars of this size. All of the steel reinforcing bars were centred in the cells and were held in place by welded wire mesh to ensure the accuracy of the placement during construction and grouting. The reinforcing steel extended 150 mm beyond the top and bottom of the specimens to accommodate mechanical couplers which provided end anchorage to ensure bond failure occurred within the lap splice region during testing. Ahmed and Feldman [2] concluded that a 300 mm contact splice length resulted in yielding of the steel reinforcement in specimens with contact lap splices similar to that shown in

Figure 2 (b). On-going work at the University of Saskatchewan conducted by Sanchez [5] showed that a 200 mm splice length would ensure that both contact and non-contact lap splices would fail in bond. This lap splice length was therefore selected for the current investigation.

Figure 3 shows the five different splice details for the specimens constructed within this investigation. Figure 3 (a) shows the splice detail for the control specimen with non-contact lap splices (NCLS). The lapped bars were centred in two outermost cells on each side, similar to the wall splice specimens used in Ahmed and Feldman's [2] investigation. Figure 3 (b) shows the splice detail for the control specimens with contact lap splices (CLS). In these specimens, the spliced bars were centred in the first interior cells. These two splice details acted as controls and allowed for a quantitative comparison of the splice resistance of the three remedial procedures to be established.

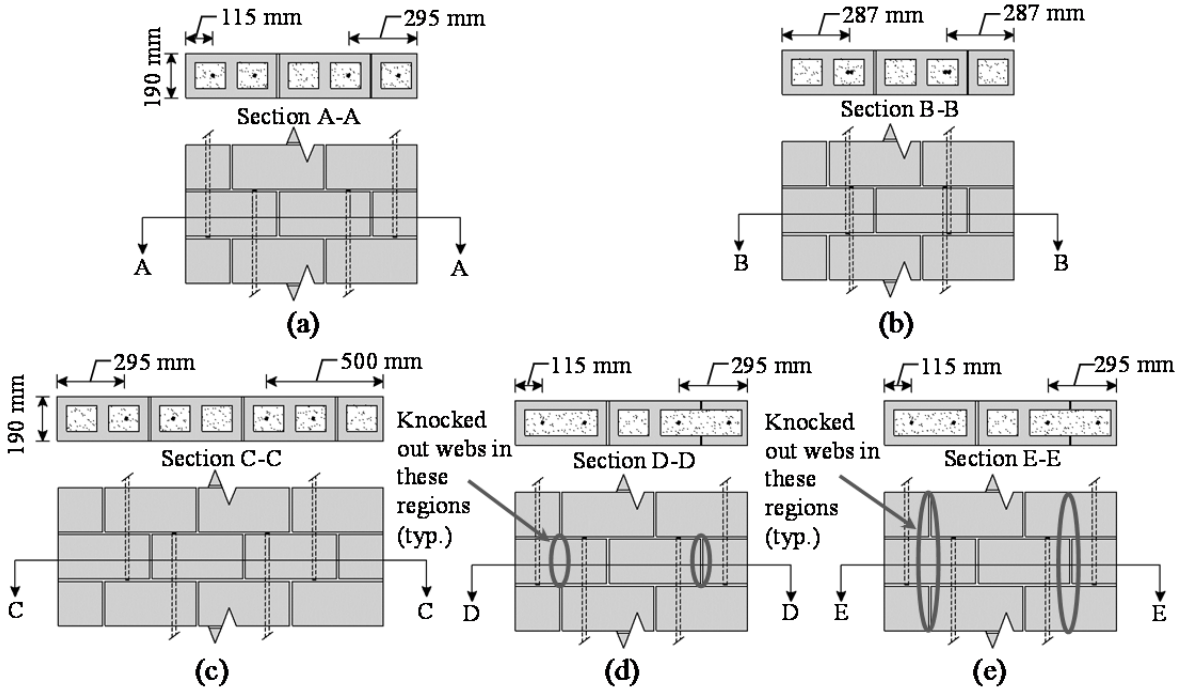

Figure 3: Splice Details for: (a) Control Specimens Featuring Non-Contact Lap Splices (NCLS), (b) Control Specimens Featuring Contact Lap Splices (CLS), (c) Remedial Technique Using Grouted Confinement Cells (GCC), (d) Remedial Technique Using a Single Course of Knockout Webs (1KO), and (e) Remedial Technique Using Three Courses of Knockout Webs (3KO)

Figures 3 (c) to (e) show the splice details for the three remedial techniques included in this study. Grouted confinement cell specimens (GCC), shown in Figure 3 (c), were 3.5 blocks wide and therefore featured an extra full concrete masonry unit width to allow for a grouted cell to be located on either side of the cells containing reinforcement. This specimen geometry was selected to determine if placing the outermost bar in the non-contact lap in the exterior cell of a specimen compromised the tensile resistance of the lap splice. Figure 3 (d) shows the splice detail for the single knock-out (1KO) remedial specimens. The lapped bars were once again located in adjacent cells and centred in the two outermost cells on each side. Section D-D in Figure 2 (d) shows that the webs separating the adjacent cells along the one course tall lap splice

length were removed. The intent of this remedial method was to eliminate grout shrinkage at the block-grout interface that leads to splitting cracking as was noted by Ahmed and Feldman [2]. Figure 3 (e) shows the splice detail for the triple knock-out (3KO) remedial specimens. These specimens are similar to the 1KO specimens; however, additional webs were removed between the lapped bars in the courses directly above and below the lap splice length, for a total of three courses of knock-out webs. These specimens increased the uninterrupted grout region between the lapped bars. This is important because the compressive struts which form between the lapped bars do so at an angle that may extend beyond the lap splice length, as shown in Figure 1.

MATERIAL PROPERTIES

Hollow concrete masonry units with frogged ends were obtained from a common batch of material via a local supplier. The concrete units were delivered to the Structures Lab two weeks prior to construction to allow for the block temperature to equilibrate with that in the laboratory. The standard concrete blocks measured 390 mm long x 190 mm wide x 190 mm high. Half blocks were created in the Structures Laboratory by cutting whole blocks in two, thus ensuring all the concrete masonry units had the same material properties. The compressive strength of the blocks was determined by using the testing protocol in ASTM standard C140-12 [6]. An average value of 19.7 MPa (COV = 11%) was calculated using the net cross-sectional block area and was based on the results of six tests.

Type S mortar was prepared in the laboratory in accordance with CSA Standard A179 [7] with Type S Mortar Cement, with a 3:1 masonry cement to sand ratio. Ninety six mortar cubes, six for every batch, were cast and tested in accordance to CSA Standard A179 [7]. The average overall compressive strength was 17.0 MPa with a coefficient of variation of 17%.

The grout was also prepared in the laboratory in accordance with CSA Standard A179 [7] and consisted of Type GU cement, aggregate with a maximum particle size of 10 mm, and a 5:1 aggregate to cement ratio by weight. A water-to-cement ratio between 0.95 and 1.00 was used in the batching process and the target slump test value immediately following batching was 250 mm. The average result from all of the slump tests was approximately 252 mm. Ninety six non-absorbent 75 mm grout cylinders (three for every batch of grout) and 32 absorbent 190 mm high x 100 mm wide grout prisms (one for every batch of grout) were cast and tested in accordance with ASTM Standard C1019-11 [8]. The average compressive strength of the non-absorbent grout cylinders and absorbent grout prisms were 14.0 MPa (COV = 15%) and 14.3 MPa (COV = 14%), respectively.

A standard fully grouted one block wide by three courses tall masonry prism was constructed alongside each wall splice specimen. The prisms were constructed and tested in accordance with CSA Standard S304.1 Annex D [1] and yielded an average compressive strength of 13.4 MPa (COV = 10%).

No. 15 Grade 400 hot-rolled deformed reinforcing bars conforming to CSA Standard G30.18 [9] were used in all of the wall splice specimens. Nine samples were acquired from the excess lengths of bars used in the wall splice specimens. Material properties were established using the tensile testing procedures outlined in ASTM Standard A370-12 [10]. The average yield strength was 442 MPa (COV = 0.65%).

SPECIMEN TESTING

Figure 4 shows that the wall splice specimens were simply supported and tested in a horizontal position under four-point loading. Steel plates placed on the end of the specimen were held in place by Type 2 ZAP Screwlock mechanical couplers as supplied by Bar Splice Products Inc. These couplers provided end anchorage for the reinforcing bars and so ensured that failure occurred within the lap splice length. Two computer controlled MTS actuators with a 300 mm stroke and a combined capacity of 1000 kN operated in deflection control at a rate of 0.5 mm per minute. A transverse spreader beam, not shown in Figure 4, was used to transfer the applied force of the two actuators to a single point at its transverse midspan. A roller was positioned below this spreader beam at midspan to eliminate the effects of any potential differences between the instantaneous deflection rates of the two actuators. A steel I-section spreader beam (shown in Figure 4) in the longitudinal direction was located between the upper transverse spreader beam and the specimen to distribute the force equally to the wall splice specimen below. An additional 0.74 kN was added to the recorded load to account for the weight of the spreader beam assembly in the subsequent numerical analysis as it was not recorded by the load cell.

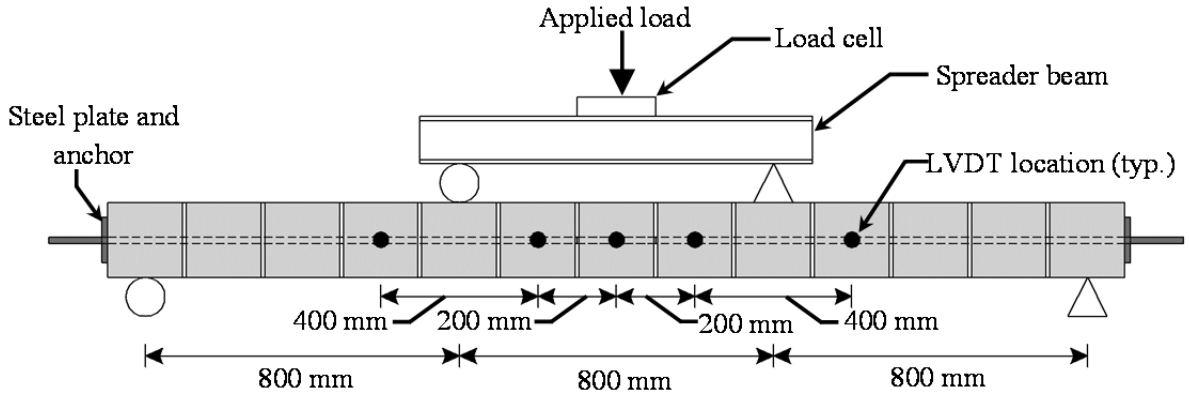

Figure 4: Loading Geometry and Instrumentation on Wall Splice Specimen

Figure 4 also shows the location of the six linear variable displacement transducers (LVDTs) which were used to measure the deflection profile of the wall splice specimen. Two LVDTs were placed at the midspan of the specimen, one on either side. The results of these two LVDTs were averaged in the subsequent analysis in an effort to obtain the most accurate measure of the midspan displacement. LVDTs were also placed 200 mm and 600 mm on either side of the specimen midspan (four in total). All of the load and displacement data was logged using a data acquisition system at a rate of 2 Hz and was controlled by a notebook computer operating Lab View™ software.

DISCUSSION OF TEST RESULTS

This section discusses the results of an analysis based of the load and LVDT data recorded during testing and summarizes visual observations in terms of internal and external damage patterns. The visual observations are used to explain the behavioural differences between the various wall splice specimens.

Table 1 shows the results of the iterative finite difference approach which was used to determine the depth of the compression zone so the tensile resistance of the reinforcement could be calculated. Curvature of the wall splice specimens was determined by plotting the deflection

profile from the six LVDTs placed along the length of the wall, while the moment was calculated based on geometry and loading of the wall splice specimen throughout testing. The analysis incorporated a Kent-Park curve [11] to model the stress versus strain response of the masonry assemblage, and required the input of the compressive strength, f'_m, as measured from the masonry prism tested in conjunction with each wall splice specimen, and the modulus of elasticity, E_m, which was determined by calculating the slope of the stress versus strain curve obtained from the same masonry prism test. The cracking load, which was determined from analysing the load-deflection response for each wall specimen, was also incorporated into the analysis, as were the average stress-strain properties of the reinforcing steel as determined from the results of the tensile tests.

Table 1: Resulting Test Data

Wall Set	Wall Number	Age @ Test [days]	Max Load [kN]	Max Midspan Moment [kNm]	Midspan Displacement @ Max Load [mm]	Tension in Spliced Reinforcing Bars [kN]	f'_m [MPa]	E_m [MPa]
NCLS	1	43	11.7	7.62	6.67	54.1	12.9	8910
	2	42	8.11	6.16	4.02	32.9	13.5	8590
	3*	49	7.57	5.95	3.15	28.6	11.9	10500
	Average		9.92	6.89	5.35	43.5	13.2	8750
	COV [%]		18.2	10.6	24.8	24.3	2.16	1.83
CLS	1	63	29.6	14.8	16.4	123	12.5	10100
	2	62	22.9	12.1	17.5	130	12.5	6890
	3	60	25.8	13.2	17.1	134	14.9	8710
	Average		26.1	13.4	17.0	129	13.3	8570
	COV [%]		10.6	8.32	2.75	3.47	8.45	15.3
GCC	1	78	12.8	8.83	7.24	65.9	14.8	7770
	2*	82	9.08	7.35	1.62	17.6	14.2	10100
	3	75	13.4	9.08	4.65	40.7	11.9	7450
	Average		13.1	8.96	5.95	53.3	13.4	7610
	COV [%]		2.41	1.40	21.8	23.6	10.9	2.10
1KO	1	67	12.2	7.80	8.89	76.5	15.9	14900
	2	69	13.3	8.24	7.01	63.7	11.7	11100
	3	70	16.5	9.51	8.62	72.8	15.2	10900
	Average		14.0	8.52	8.17	71.0	14.3	12300
	COV [%]		13.0	8.51	10.2	7.58	12.8	15.0
3KO	1	54	17.5	9.92	10.9	83.0	12.9	7210
	2	57	17.6	9.96	9.44	75.8	14.4	10900
	3	50	15.7	9.20	9.12	70.3	11.5	9990
	Average		16.9	9.69	9.81	76.3	12.9	9370
	COV [%]		5.13	3.60	7.80	6.81	9.19	16.8

*Physical outliers as identified in the accompanying text. The resulting data from these specimens have been excluded in the averages and coefficients of variation as reported.

Visual observations of the different wall splice specimens provided a better understanding of their overall performance and an indication of their failure mode. Figure 5 (a) shows the presence of a void between the frogged-end blocks and cracking along the grout-block interface which were typical of both the control NCLS specimens and the remedial GCC specimens. These features limit the shear component of the compressive struts between lapped bars shown in Figure 1 and result in reduced tensile capacity of typical non-contact lap splices where the lapped bars are placed in adjacent cells. These observations are similar to those made by Ahmed and Feldman [2] and suggest that splitting contributes to the failure mode of wall splice specimens with non-contact lap splices. Figure 5 (b) shows that good grout consolidation was achieved between the lapped bars in specimens featuring knock-out webs in the lap splice length. This increased the capacity of the shear component of the compressive struts, thus allowing for a more effective transfer of tensile forces between lapped bars. Figure 5 (c) shows the typical damage resulting from the testing of the CLS specimens. The gaps at the end of the reinforcement suggest a bond failure due to end slip of the reinforcing bars. The primary internal cracking occurred at the bed joints, in the same plane where the lapped reinforcing bars terminated. Figures 5 (a) and (b) also show cracking at this same location, due to the location of the cut ends of the lapped bars terminating at bed joints and thus reducing the flexural capacity of these specimens. This phenomenon is a peculiarity that must be considered when evaluating bond in masonry construction given it reduced the tensile capacity reinforcement. This situation, however, was common to all the wall specimens included in this investigation and so the results could still be directly compared.

Visual observations were also used to identify test specimens NCLS#3 and GCC #2 as physical outliers and so excluded their resulting test data from the calculations of the average values of their respective wall sets. Significant voids between the grout and the reinforcing steel within the lap splice length were identified, causing a reduced overall load resistance of these specimens, and so a reduced tensile resistance of the reinforcement.

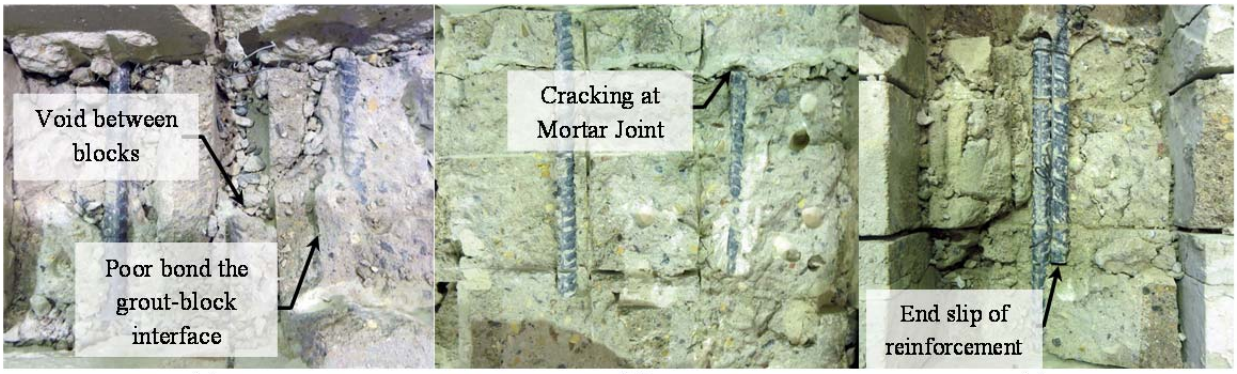

Figure 5: Typical Visual Observations of Internal Distresses: (a) NCLS and GCC Specimens, (b) 1KO and 3KO Specimens, and (c) CLS Specimens.

Figure 6 shows comparison of the calculated tensile resistance of all wall splice specimens following testing. The average tensile resistance of the lapped bars in the NCLS and CLS control specimen sets were 43.5 kN (COV = 24.3%) and 129 kN (COV = 3.47%) respectively. This equated to a 197% increase in splice capacity and an 85.7% decrease in the coefficient of variation between control wall sets. The higher coefficient of variation for the NCLS results can

be attributed to their failure mode, which involved splitting due to the poor bond at the grout-block interface as compared to the pull-out of the reinforcement in specimens with contact lap splices (CLS). Failures which involve pull-out of the steel reinforcement have lower coefficients of variation because the failure mode is mainly dependant on the overlap of the spliced bars, while splitting failure is dependent on the highly variable tensile properties of the cementious materials.

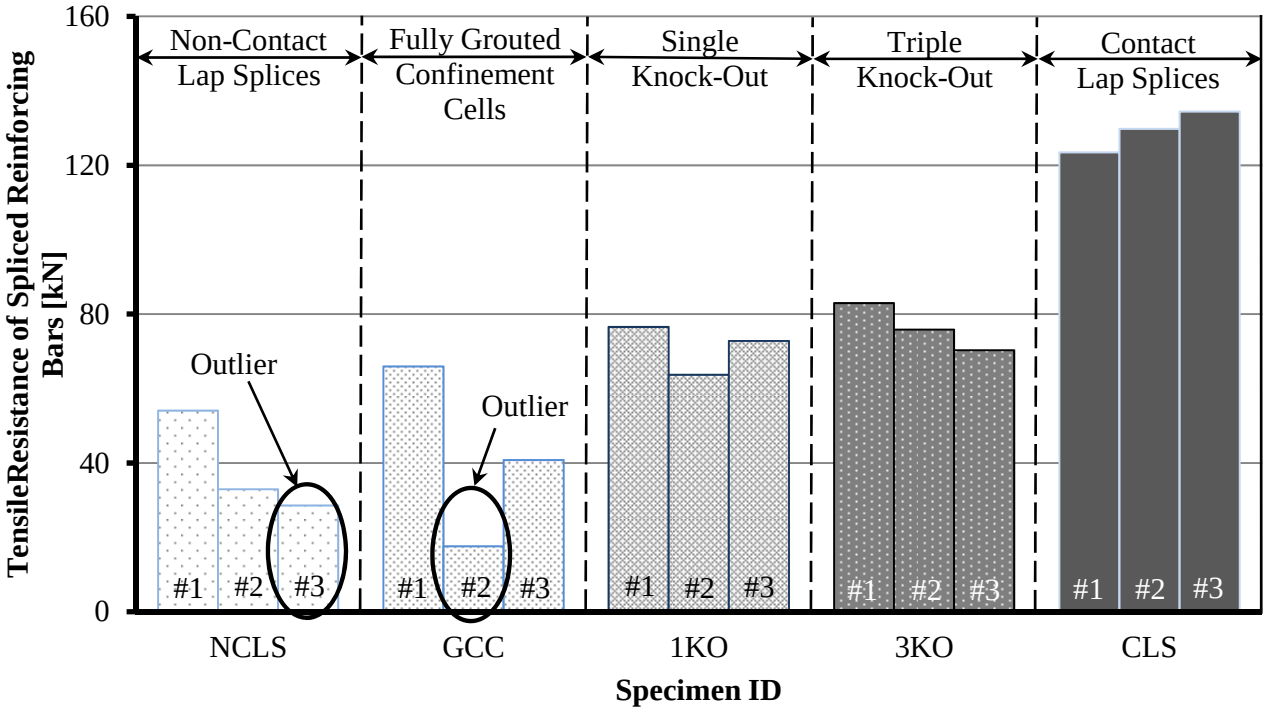

Figure 6: Comparison of the Tensile Resistance of the Different Wall Splice Specimen Sets.

Figure 6 also shows that wider GCC specimens resulted in slightly higher tensile resistance in the lapped reinforcement as compared to the control NCLS wall splice specimens. The additional mass due to the increased specimen width resulted in added confinement which delayed splitting cracks from forming between the lapped bars. However, the coefficients of variation remained virtually the same due to the failure mode of the NCLS specimens which involved poor bond at the interface between the grout and the block. The 1KO specimens showed a 63.2% increase in splice capacity and a 68.8% decrease in the coefficient of variation as compared to the NCLS control specimens. This decreased coefficient of variation is due to the elimination of the grout-block interface between the lapped reinforcing bars.

The 3KO wall splice specimens yielded the highest tensile capacities of the three evaluated remedial techniques, with a 74.5% increase in the tensile capacity of the lapped bars and a 72.0% decrease in the coefficient of variation as compared to the NCLS specimens. The increase in the tensile capacity of the 1KO and 3KO specimens is a result of the elimination of the grout-block interface located between the lapped bars. The 3KO specimens performed better than the 1KO specimens because the additional removal of the grout-block interface in the courses directly

above and below the splice allowed for an increased effective lap length since more diagonal compressive struts could effectively form between the two lapped bars.

The remedial techniques tested thus far showed improvement in the tensile capacity of non-contact lap spliced reinforcing bars, but did not increase the resistance to match that of lapped bars in contact. The second phase of testing will feature an evaluation of additional remedial techniques in the expectation that further increases in tensile capacity can be achieved.

CONCLUSIONS

This paper presents the results of an experimental program consisting of two sets of control specimens and three sets of specimens featuring remedial techniques, for a total of 15 specimens. The three different remedial methods were tested to determine if the tensile resistance of the non-contact lapped bars could be increased to match that of bars in contact since non-contact lap splices are often required in masonry construction. All specimens were reinforced with No. 15 reinforcing bars with 200 mm long lap splice lengths. The following conclusions were noted:

1. Crack patterns suggest that the spliced bars with a 200 mm lap length resulted in the termination of the reinforcement along a bed joint and thus reduced specimen capacity as compared to that which would have occurred if the cut ends of the bars occurred within a concrete masonry unit.

2. The wall splice specimens featuring three courses of knock-out webs resulted in the greatest improvement in the tensile capacity of the lapped bars of all three remediation procedures evaluated in this investigation. Removal of the block webs between the lapped bars, which eliminated the poor bond known to exist at the grout-block interface, increased the tensile capacity of the spliced bars up to 74.5% compared to the control specimens featuring non-contact lap splices, where the lapped bars were in adjacent cells.

3. The coefficients of variation for specimens with one and three courses of knock-out webs in the splice region decreased by 68.8% and 72.0% respectively as compared to the control specimens with non-contact lap splices. This was due to the elimination of splitting cracking caused by poor bond at the grout-block interface which is dependent on the highly variable tensile properties of cementious materials. Splitting cracking was not eliminated in the wall splice specimens featuring grouted confinement cells, and, as a result, the coefficient of variation remained unchanged as compared to the control wall splice specimens with non-contact lap splices.

ACKNOWLEDGEMENTS

The authors gratefully acknowledge the assistance of Brennan Pokoyoway and Dale Pavier, University of Saskatchewan Structures Laboratory Technicians; journeyman mason Roy Nicolas, Gracom Masonry; and fellow graduate students for assistance with preparation and testing of all specimens. Financial Support was provided by the Canadian Masonry Design Centre, the Saskatchewan Masonry Institute, NSERC Canada, and the University of Saskatchewan.

REFERENCES

1. Canadian Standards Association. (2004) “CAN/CSA S304.1-04 Design of Masonry Structures” CSA, Rexdale, Ontario, Canada.
2. Ahmed, K., Feldman, L.R. (2012) “Evaluation of Contact and Noncontact Lap Splices in Concrete Block Masonry Construction” Canadian Journal of Civil Engineering, Vol. 39 Issue 5, pp 515-523.
3. Sagan, B.E., Gergely, P., While, R.N., (1991) “Behavior and Design of Non-Contact Lap Splices Subjected to Repeated Inelastic Tensile Loading” ACI Structural Journal, Vol. 88, No.4 pp 420-431.
4. Bischoff, P.H., Moxon, D., (2005) “Shrinkage Wreaks Havoc with Tension Stiffening in Reinforced Masonry Test Specimens” Proceedings of the 9th Canadian Masonry Symposium, Fredericton, New Brunswick, Canada.
5. Sanchez, D. (2011-2012) “The Effect of Splice Length and Distance Between Lapped Reinforcing Bars In Concrete Block Specimens” Personal Communications, University of Saskatchewan, Saskatoon, Saskatchewan, Canada.
6. ASTM International. (2012) “C140-12 Standard Test Methods for Sampling and Testing Concrete Masonry Units and Related Units” ASTM Standards, West Conshohocken, PA, USA.
7. Canadian Standards Association. (2004) “CAN/CSA A371-04 Masonry Construction for Building” CSA, Rexdale, Ontario, Canada.
8. ASTM International. (2012) “C1019-12 Standard Test Method for Sampling and Testing Grout” ASTM Standards, West Conshohocken, PA, USA.
9. Canadian Standards Association. (2009) “CAN/CSA G30.18-09 Carbon Steel Bars for Concrete Reinforcement” CSA, Rexdale, Ontario, Canada.
10. ASTM International. (2012) “A370-12 Standard Test Methods and definitions for Mechanical Testing of Steel Products” ASTM Standards, West Conshohocken, PA, USA.
11. Kent, D.C., Park, R. (1971) “Flexural Members with Confined Concrete” Journal of the Structural Division, ASCE, Vol. 97, No. ST7, pp 1969-1990.